

Pulsar-Wind Nebulae as a Dominant Population of Galactic VHE Sources

TeV particle Astrophysics
08/26/2013

Blagoy Rangelov
The George Washington University

Collaborators:

Oleg Kargaltsev (The George Washington University)

George Pavlov (Penn State University)

Outline

- Overview
- Galactic very high energy (VHE) sources
- Pulsar-wind nebulae (PWNe)
- Other confirmed VHE sources
- Unidentified and “dark” VHE sources

Overview

- Review of properties of Galactic VHE sources detected at TeV energies
- The number of associations between the VHE sources and pulsars has grown in recent years, making PWNe the dominant population
- Supernova remnants (SNRs) and high-mass X-ray binaries (HMXBs) are the other two well-established classes of Galactic VHE sources
- There is a number of VHE sources which remain to be identified, including a few “dark” sources which do not show plausible counterparts at any other wavelengths

Higher energies (GeV and TeV)



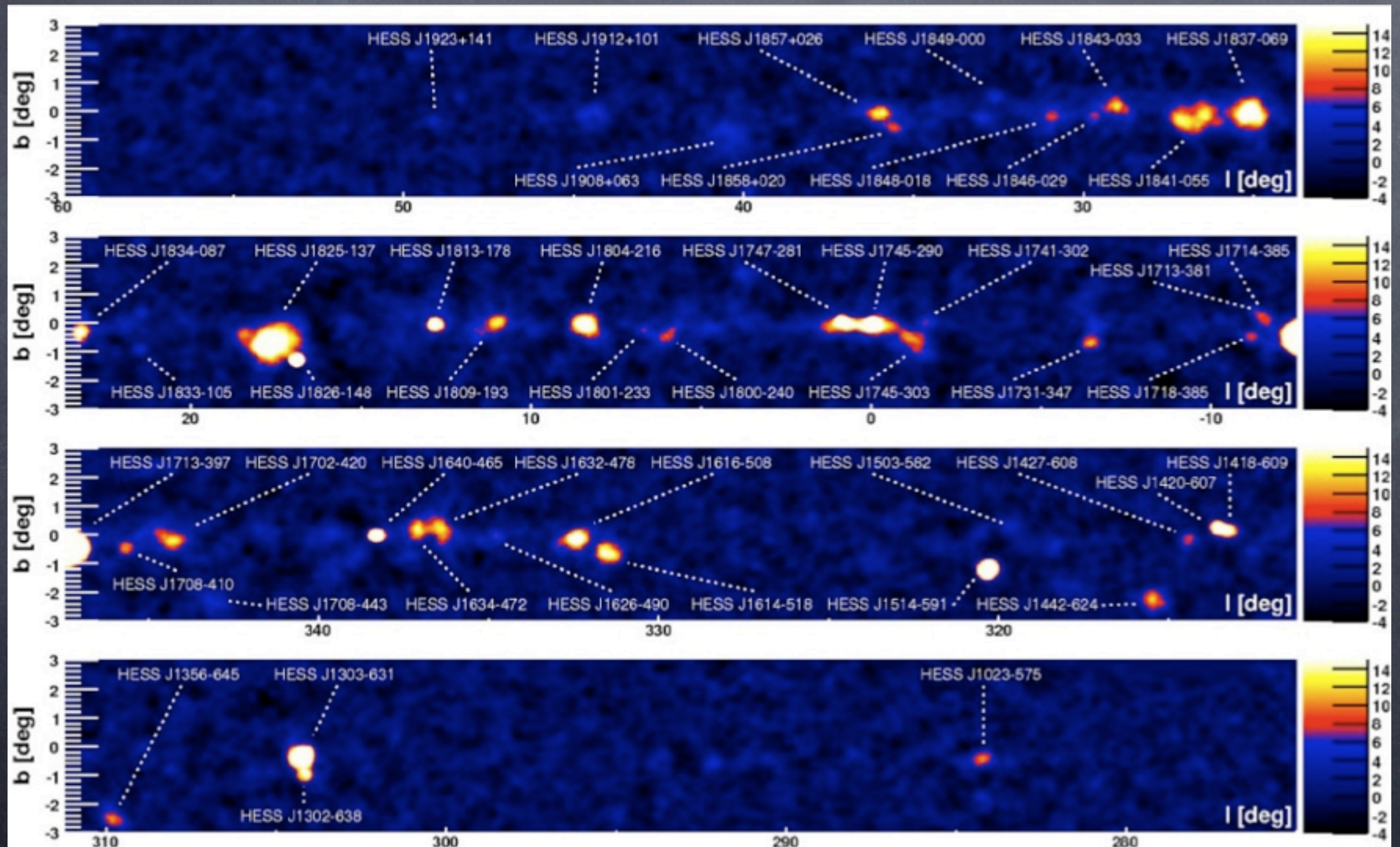
VERITAS

Fermi



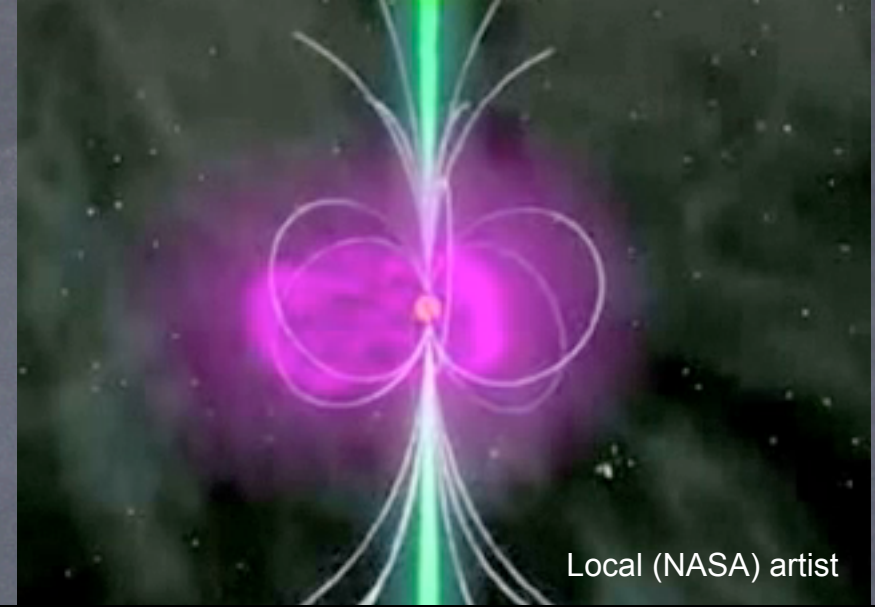
H.E.S.S.

Many extended TeV sources have
been resolved

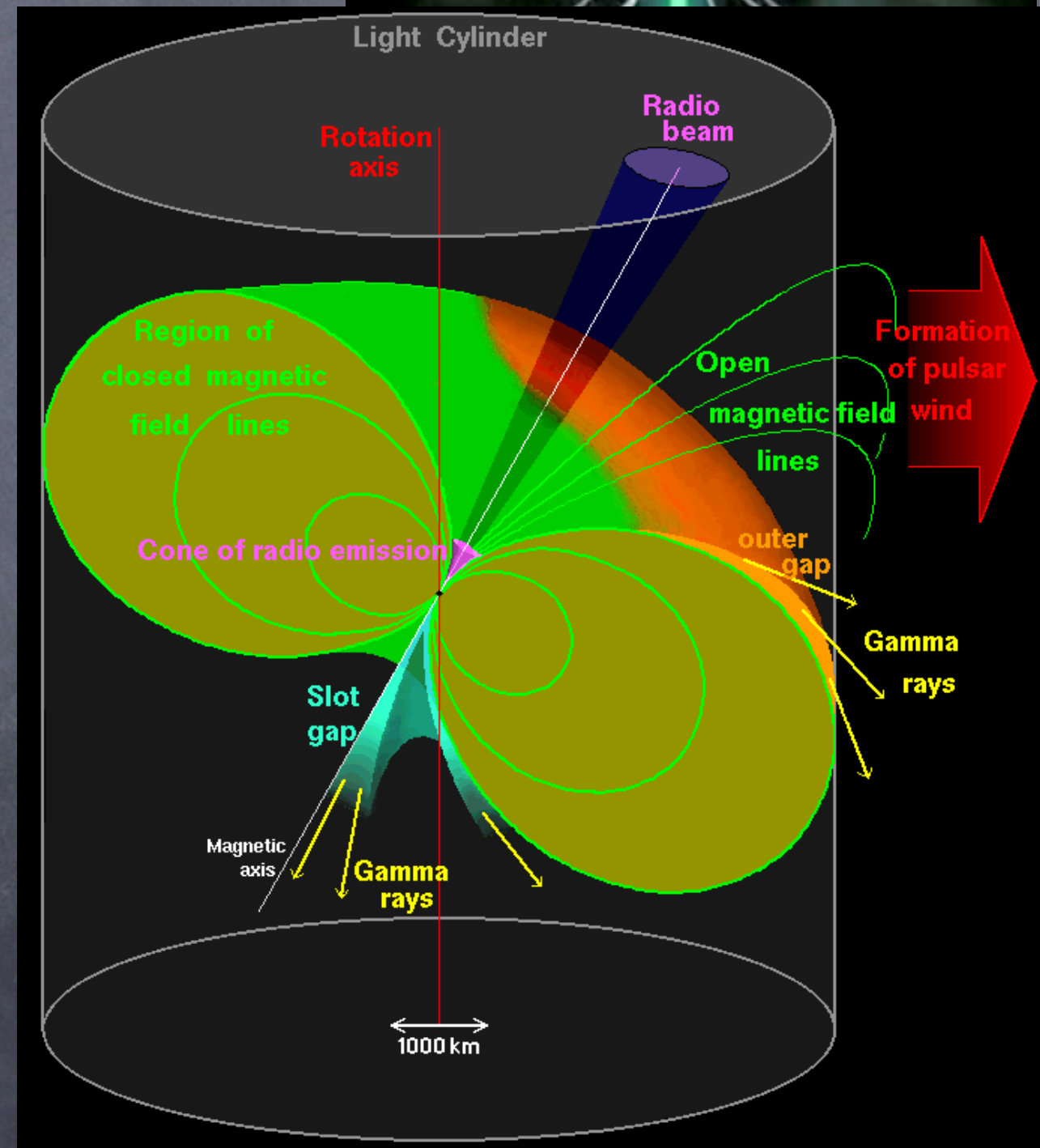


Pulsars

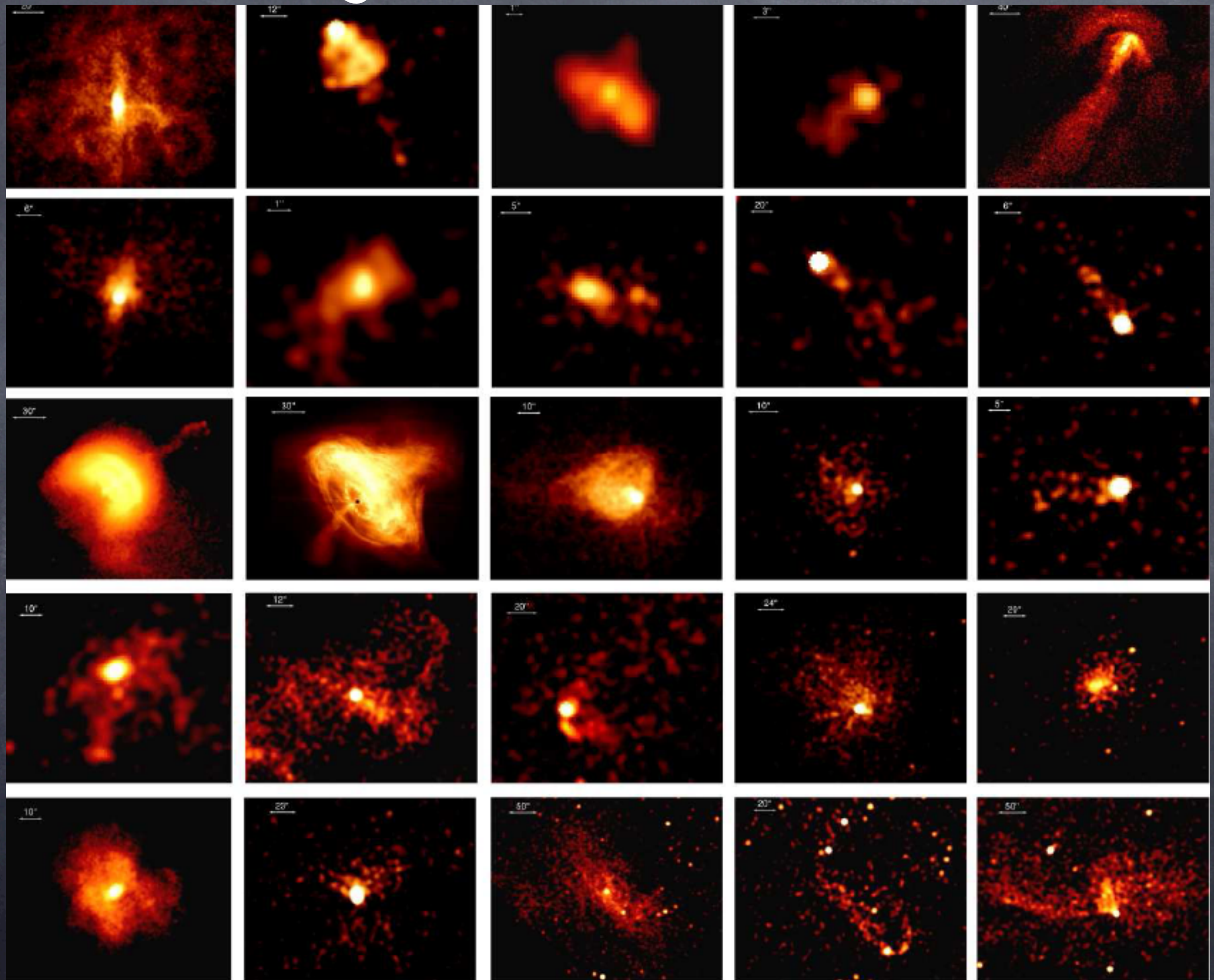
- Pulsars are neutron stars (NSs) with active magnetospheres populated by ultra-relativistic particles emitting non-thermal radiation (synchrotron, curvature, inverse Compton).
- Power Source: NS rotation - $\dot{\mathcal{E}}$
- Emitted fraction of $\dot{\mathcal{E}}$
 - $<0.001\%$ - radio
 - $\sim 0.01\text{--}10\%$ - X-rays and gamma-rays
 - the rest is pulsar wind!



Local (NASA) artist

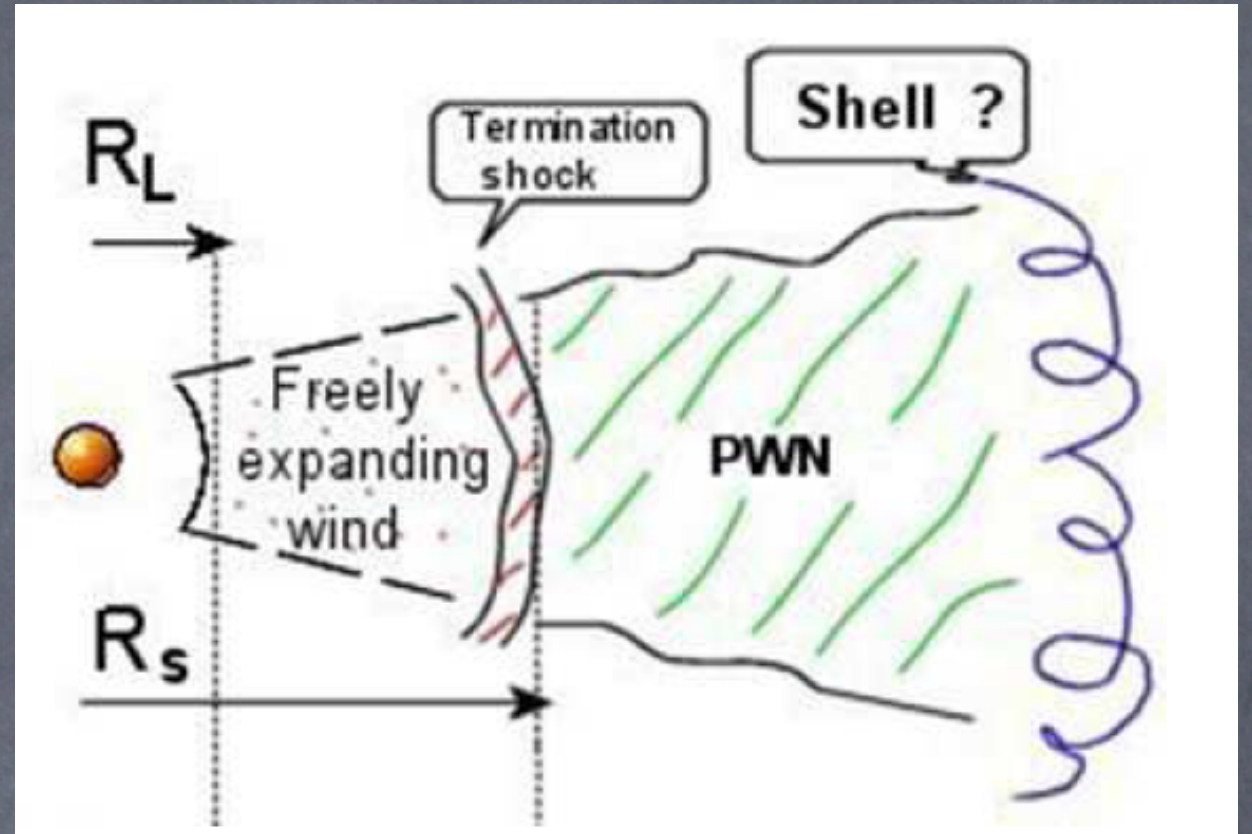


Chandra images of PWNe



Pulsar-Wind Nebulae

- This cartoon assumes axisymmetric wind expansion which may not be the case due to the interaction with ISM
- Fast moving pulsars are accompanied by bowshocks, others show jets and torii.
- If the SNR shock becomes asymmetric (due to the interaction with the environment) the reverse shock will also be asymmetric and can “crush” a PWN pushing it to the side from the pulsar
- Two distinct PWN parts:
 - “relic” PWN filled with aged pulsar wind particles (cold, faint X-ray, TeV emitters)
 - compact “fresh” PWN



Cooling Times

- Typical energies of the synchrotron or inverse Compton scattering (ICS) photons (E_{syn} and E_{ICS}) depend on the energy of emitting electrons, the magnetic field or the energy of seed photon

$$E_{\text{syn}} \sim 4(E_e/100 \text{ TeV})^2 (B/10^{-5} \text{ G}) \text{ keV}$$
$$E_{\text{ICS}} \sim 1(E_e/20 \text{ TeV})^2 (\epsilon/6 \times 10^{-4} \text{ eV}) \text{ TeV}$$

$$E_{\text{syn}} \sim 0.18(E_{\text{ICS}}/1 \text{ TeV})(B/10^{-5} \text{ G})(\epsilon/6 \times 10^{-4} \text{ eV})^{-1} \text{ keV}$$

- The synchrotron and ICS+synchrotron cooling times

$$\tau_X \approx 1.2 B_{-5}^{-3/2} (E_{\text{syn}}/1 \text{ keV})^{-1/2} \text{ kyr}$$
$$\tau_\gamma \approx 100(1 + 0.144 B_{-6}^2)^{-1} (E_{\text{ICS}}/1 \text{ TeV})^{-1/2} \text{ kyr}$$

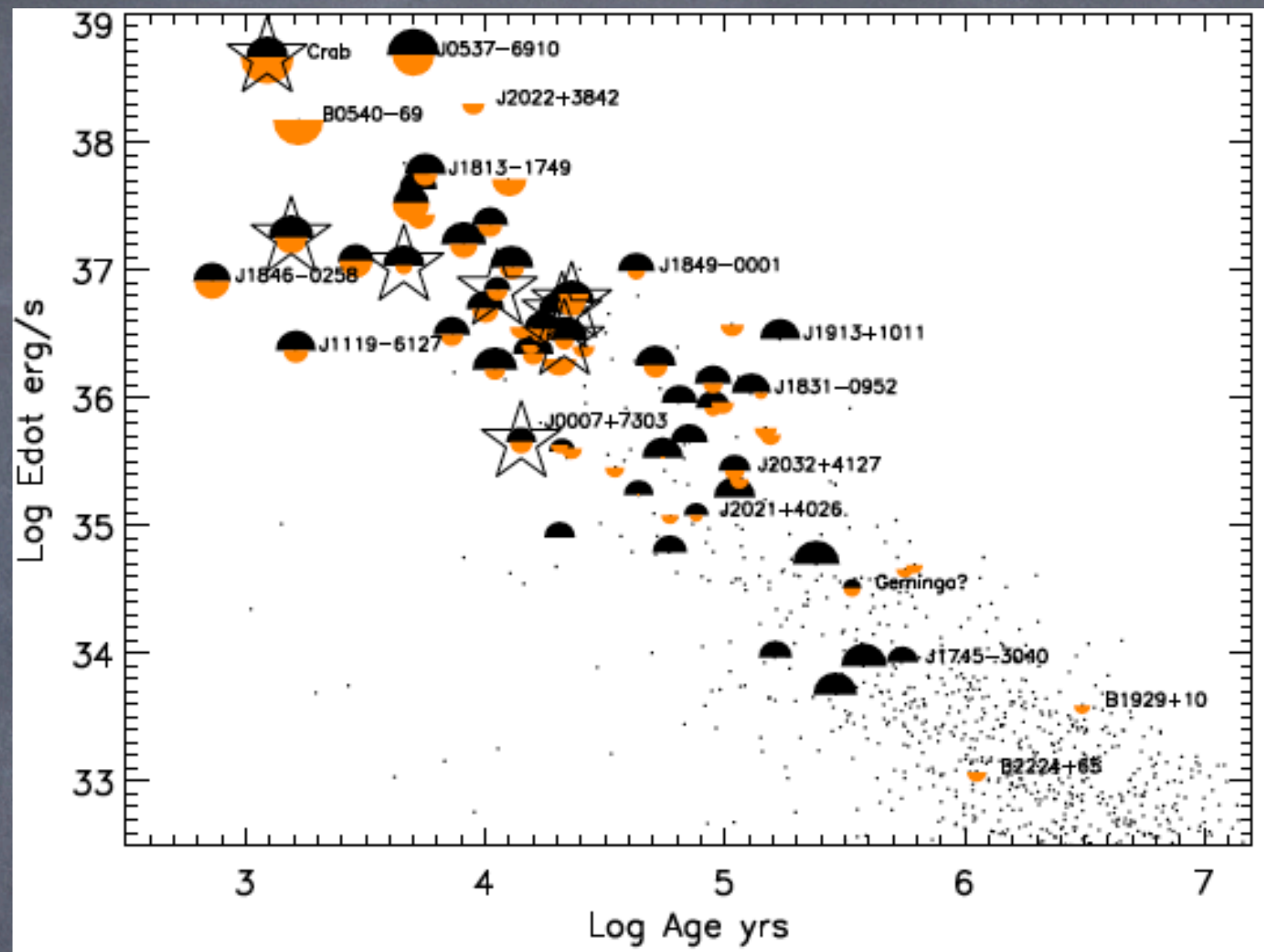
- The cooling times and the luminosities of X-ray and TeV PWNe also depend on other factors, such as the presence of local sources of IR photons, the size of the region from which luminosities are measured, and the validity of the Thomson regime approximation.

Pulsar-Wind Nebulae

- 91 known PWNe or PWNe candidates
- For some PWNe no pulsar have been detected yet
- Only 52 have (possible) VHE counterpart
- Establishing association between VHE source and PWN/pulsar is a complex task

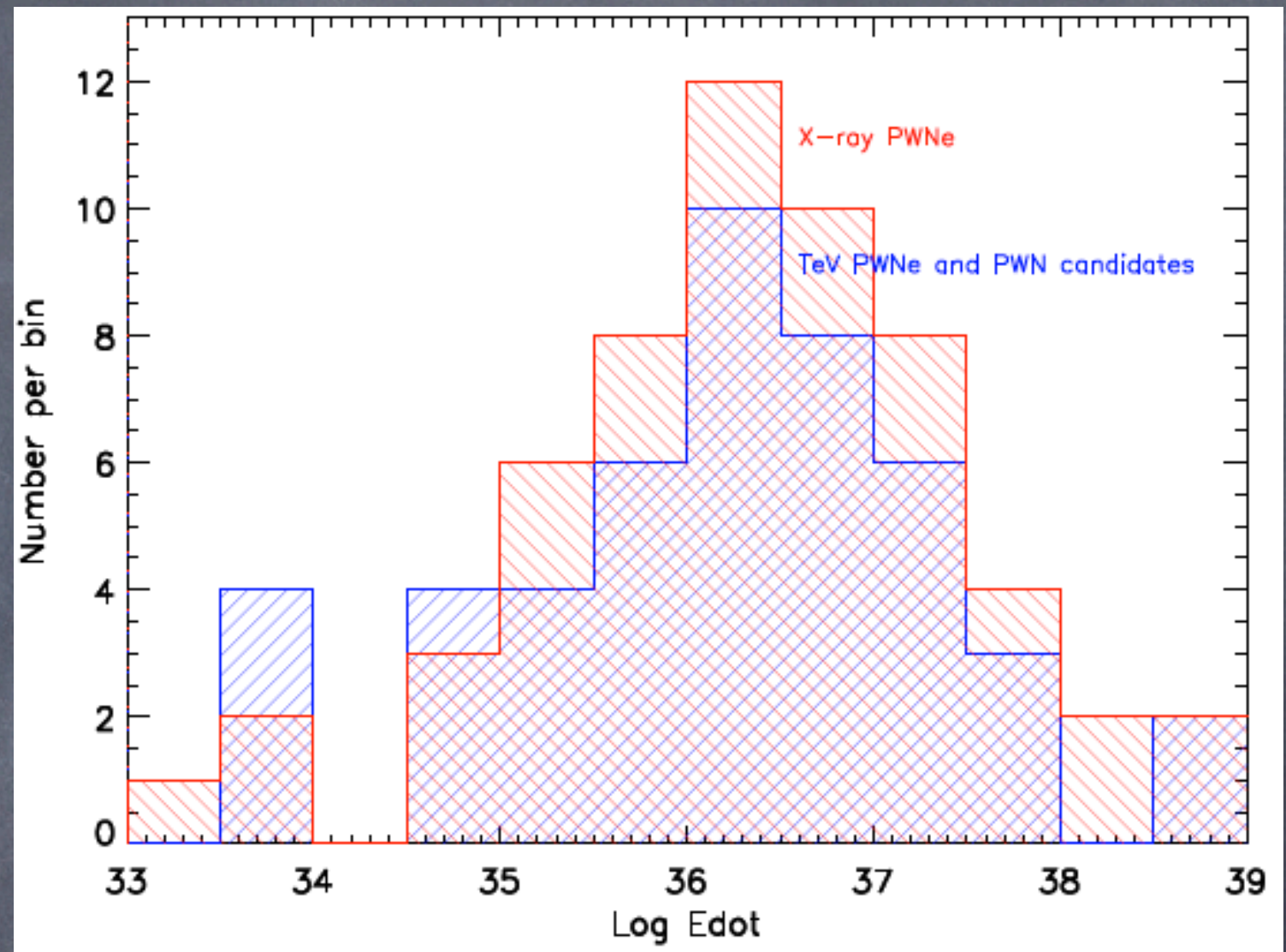
| # | PSR | PWN* | VHE src. [†] | log E [erg/s] | log τ [yr] | d** kpc | Rad./H _a /GeV [†] |
|----|-------------|---------------------------|----------------------------|------------------|---------------|-------------------|---------------------------------------|
| 1 | J0537-6910 | N157B | H J0537-691 | 38.68 | 3.70 | 50 | Y/N/N |
| 2 | B0531+21 | Crab | H J0534+220 | 38.66 | 3.09 | 2 | Y/N/Y |
| 3 | J2022+3842 | G76.9+1.0 | ... | 38.30 | 3.95 | 8 | Y/N/N |
| 4 | B0540-69 | N158A | ... | 38.17 | 3.22 | 50 | Y/N/N |
| 5 | J1813-1749 | G12.82-0.02 | H J1813-178 [?] | 37.75 | 3.75 | 4.5 | N/N/N |
| 6 | J1400-6325 | G310.6-1.6 | ... | 37.71 | 4.10 | 6 | Y/N/N |
| 7 | J1833-1034 | G21.50-0.89 | H J1833-105 | 37.52 | 3.69 | 4.8 | Y/N/N |
| 8 | J0205+6449 | 3C 58 | ... | 37.43 | 3.73 | 3.2 | Y/N/N |
| 9 | J2229+6114 | G106.65+2.96 | V J2228+609 | 37.35 | 4.02 | 3 | Y/N/N |
| 10 | B1509-58 | Jellyfish | H J1514-591 | 37.25 | 3.19 | 5 | P/N/Y |
| 11 | J1617-5055 | G332.50-0.28 | H J1616-508 [?] | 37.20 | 3.91 | 6.5 | N/N/N |
| 12 | J1124-5916 | G292.04+1.75 | ... | 37.07 | 3.46 | 6 | Y/N/N |
| 13 | J1930+1852 | G54.10+0.27 | V J1930+188 | 37.06 | 3.46 | 6.2 | Y/N/N |
| 14 | J1420-6048 | G313.54+0.23 | H J1420-607 | 37.02 | 4.11 | 5.6 | P/N/N |
| 15 | J1846-0258 | Kes 75 | H J1846-029 | 36.91 | 2.86 | 6 ^{??} | Y/N/N |
| 16 | B0833-45 | Vela | H J0835-455 | 36.84 | 4.05 | 0.29 ^P | Y/N/Y |
| 17 | J1811-1925 | G11.18-0.35 | ... | 36.81 | 4.37 | 5 | Y/N/N |
| 18 | J1838-0655 | G25.24-0.19 | H J1837-069 | 36.74 | 4.36 | 7 | N/N/Y |
| 19 | J1418-6058 | Rabbit | H J1418-609 | 36.69 | 4.00 | 3 [?] | Y/N/N |
| 20 | J1856+0245 | G36.01+0.06 [?] | H J1857+026 | 36.66 | 4.32 | 9 | N/N/Y |
| 21 | B1951+32* | G68.77+2.82 | ... | 36.57 | 5.03 | 2.5 | Y/Y/N |
| 22 | J1826-1256* | Eel | ... | 36.55 | 4.15 | 7 [?] | P/N/N |
| 23 | J2021+3651 | G75.23+0.12 | M J2019+37 [?] | 36.53 | 4.23 | 4 | N/N/N |
| 24 | B1706-44 | G343.10-2.69 | H J1708-443 | 36.53 | 4.24 | 2 | Y/N/N |
| 25 | J1357-6429 | G309.92-2.51 | H J1357-645 | 36.49 | 3.86 | 2.5 | P/N/N |
| 26 | J1913+1011 | G44.48-0.17 [?] | H J1912+101 | 36.46 | 5.23 | 4.5 | N/N/N |
| 27 | J1907+0602 | G40.16-0.89 [?] | H J1908+063 [?] | 36.45 | 4.28 | 3.2 | N/N/N |
| 28 | B1823-13 | G18.00-0.69 | H J1825-137 | 36.45 | 4.33 | 4 | N/N/Y |
| 29 | B1757-24* | Duck | ... | 36.41 | 4.19 | 5 | Y/N/N |
| 30 | J1016-5857 | G284.08-1.88 | H J1018-589B [?] | 36.41 | 4.32 | 3 | N/N/N |
| 31 | J1747-2958* | Mouse | ... | 36.40 | 4.41 | 5 | Y/N/N |
| 32 | J1119-6127 | G292.15-0.54 | H J1119-615 [?] | 36.37 | 3.21 | 8.4 | N/N/N |
| 33 | B1800-21 | G8.40+0.15 | H J1804-216 [?] | 36.34 | 4.20 | 4 | N/N/N |
| 34 | B1046-58* | G287.42+0.58 | ... | 36.30 | 4.31 | 3 | N/N/N |
| 35 | J1809-1917 | G11.09+0.08 | H J1809-193 | 36.25 | 4.71 | 3.5 | P/N/N |
| 36 | J1301-6305 | G304.10-0.24 | H J1303-631 [?] | 36.22 | 4.04 | 7 | N/N/N |
| 37 | J1718-3825 | G348.95-0.43 | H J1718-385 [?] | 36.11 | 4.95 | 4 | N/N/N |
| 38 | J1531-5610 | G323.89+0.03 | ... | 35.96 | 4.99 | 3 | N/N/N |
| 39 | J1509-5850* | G319.97-0.62 | ... | 35.71 | 5.19 | 4 | P/N/N |
| 40 | J1857+0143 | G35.17-0.57 [?] | H J1858+020 [?] | 35.65 | 4.85 | 5.5 | N/N/N |
| 41 | J0007+7303 | CTA 1 | V J0006+729 | 35.65 | 4.15 | 1.4 | N/N/Y |
| 42 | B1853+01 | G34.56-0.50 | ... | 35.63 | 4.31 | 3 | Y/N/N |
| 43 | J1809-2332 | Taz | ... | 35.60 | 4.36 | 2 | Y/N/N |
| 44 | J1958+2846 | G65.89-0.37 [?] | M J1954+28 | 35.58 | 4.32 | 2 [?] | N/N/N |
| 45 | J1702-4128 | G344.74+0.12 | H J1702-420 [?] | 35.53 | 4.74 | 5 | N/N/N |
| 46 | J0729-1448 | G230.39-1.42 | ... | 35.45 | 4.54 | 4 | N/N/N |
| 47 | J2032+4127 | G80.22+1.02 | V J2032+415 | 35.43 | 5.04 | 1.7 | N/N/N |
| 48 | J1740+1000 | G34.01+20.27 | ... | 35.36 | 5.06 | 1.4 | P/N/N |
| 49 | J0631+1036 | G201.22+0.45 [?] | M J0630+10 [?] | 35.24 | 4.64 | 3.6 | N/N/N |
| 50 | B1957+20* | G59.20-4.70 | ... | 35.20 | 9.18 | 2.5 | N/Y/N |
| 51 | J0633+0632 | G205.10-0.93 | ... | 35.08 | 4.77 | 1.5 [?] | N/N/N |
| 52 | J1740-3015 | G358.29+0.24 [?] | H J1741-302 | 34.91 | 4.31 | 3 | N/N/N |
| 53 | J0538+2817 | G179.72-1.69 | ... | 34.69 | 5.79 | 1.47 ^P | N/N/N |
| 54 | B0355+54* | Mushroom | ... | 34.66 | 5.75 | 1.04 ^P | N/N/N |
| 55 | J0633+1746* | Geminga | M J0632+17 [?] | 34.51 | 5.53 | 0.25 ^P | N/N/N |
| 56 | J1745-3040 | G358.55-0.96 [?] | H J1745-305 [?] | 33.93 | 5.74 | 2 | N/N/N |
| 57 | J1502-5828 | G319.39+0.13 [?] | H J1503-582 [?] | 33.68 | 5.46 | 8 | N/N/N |
| 58 | B1929+10 | G47.38-3.88 | ... | 33.59 | 6.49 | 0.36 ^P | P/N/N |
| 59 | B2224+65* | Guitar | ... | 33.07 | 6.05 | 1.5 | N/Y/N |
| 60 | J1747-2809 | G0.9+0.1 | H J1747-281 | 37.63 | 3.72 | 8.5 | Y/N/N |
| 61 | J1023-5746 | G284.19-0.39 [?] | H J1023-575 [?] | 37.03 | 3.66 | 8 | N/N/P |
| 62 | J1849-0001 | G32.64+0.53 | H J1849-000 | 36.99 | 4.63 | 7 | N/N/N |
| 63 | J1437-5959* | G315.78+0.2 | ... | 36.15 | 5.06 | 10 | Y/N/N |
| 64 | J0855-4644 | G266.97-1.00 | H J0852-463 [?] | 36.04 | 5.15 | 0.75 | N/N/N |
| 65 | J1831-0952 | G21.88-0.10 | H J1831-098 | 36.04 | 5.11 | 4.3 | N/N/N |
| 66 | J1459-6053 | G317.89-1.79 | H J1458-608 | 35.96 | 4.81 | 4 | N/N/N |
| 67 | J1028-5819 | G285.06-0.5 | H J1026-582 [?] | 35.92 | 4.95 | 2.3 | N/N/N |
| 68 | B1830-08 | G23.5+0.1 | ... | 35.76 | 5.17 | 5 | P/N/N |
| 69 | J1853-0004 | ... | H J1852-000 [?] | 35.32 | 5.46 | 7 | N/N/N |
| 70 | J1648-4611 | ... | H J1646-458B [?] | 35.22 | 5.04 | 5 | N/N/N |
| 71 | J2021+4026 | G78.23+2.09 [?] | V J2019+407 [?] | 35.08 | 4.88 | 1.5 | N/N/N |
| 72 | J1801-2304 | ... | H 1801-233 [?] | 34.79 | 4.77 | 4 | N/N/N |
| 73 | J1632-4757 | ... | H J1632-478 ^{??} | 34.70 | 5.38 | 7 | N/N/? |
| 74 | J1832-0827 | ... | H J1832-084 [?] | 33.97 | 5.21 | 5 | N/N/N |
| 75 | J1613-5211 | ... | H J1614-518 ^{??m} | 33.90 | 5.58 | 6 | N/N/N |
| 76 | J2124-3358 | G10.92-45.43 | ... | 33.83 | 9.58 | 0.25 | N/Y/N |

- X-ray PWNe tend to be brighter around young pulsars
- Old PWN may be seen only in TeV (the relic part) - no obvious correlation with age
- Characteristic cooling time of "relic" PWNe (due to ICS of CMB photons) ~ 100 kyr



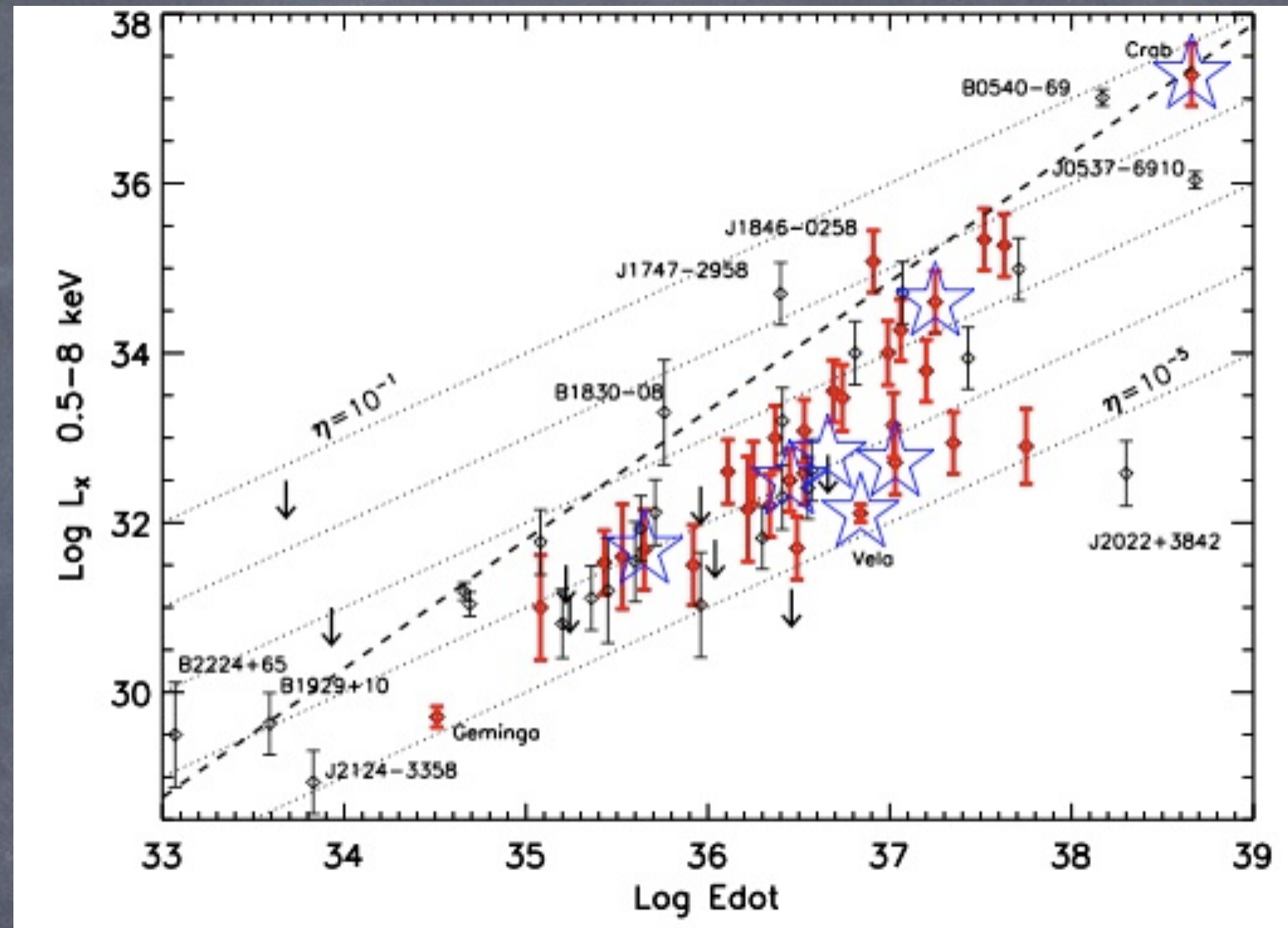
The semi-circles correspond to X-ray (orange) and TeV (black) PWNe, their sizes are proportional to logarithms of the corresponding PWN luminosities. The small black dots denote the pulsars from the ATNF catalog.

- Several energetic pulsars with prominent X-ray PWNe are not detected as TeV sources
- X-ray and TeV PWNe have similar distributions over \dot{E}
- Other factors (background photon density and compression of reverse shock) more important for the TeV PWNe than power output \dot{E}

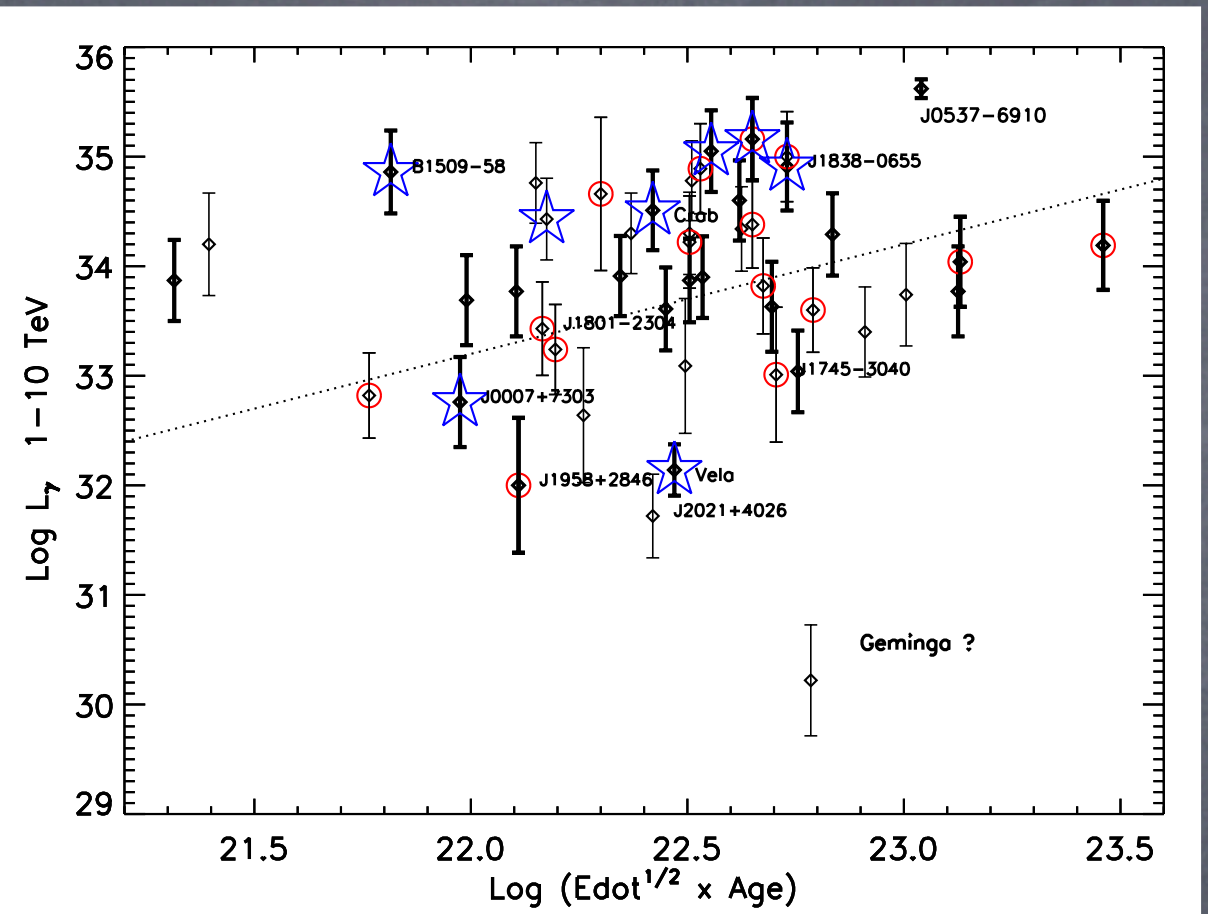
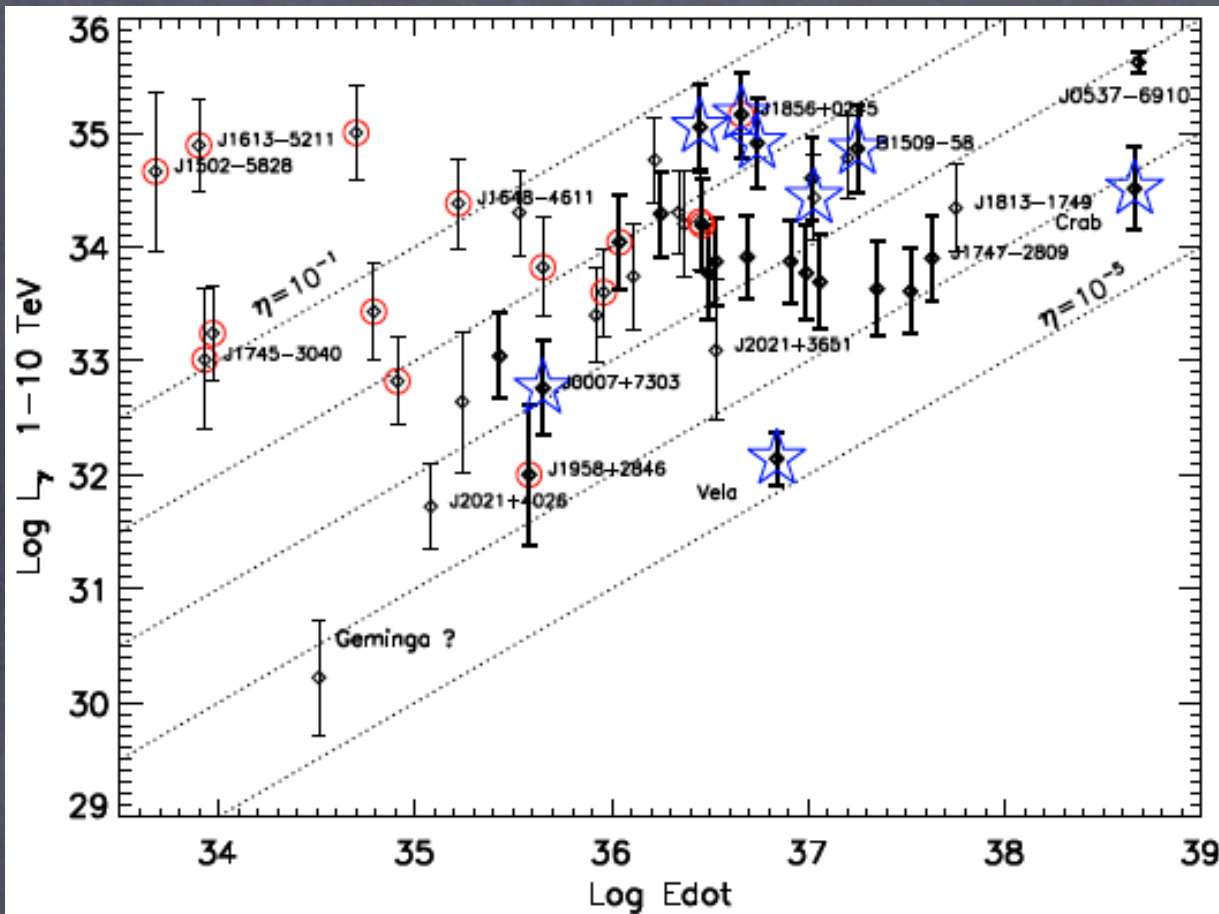


Distribution of X-ray (red) and TeV (blue) PWN and PWN candidates over pulsar's \dot{E} .

- X-ray luminosities show some correlation with \dot{E} although with very large spread for pulsars with $\dot{E} > 10^{36}$ erg/s
- L_X - \dot{E} distribution has fairly well defined upper bound



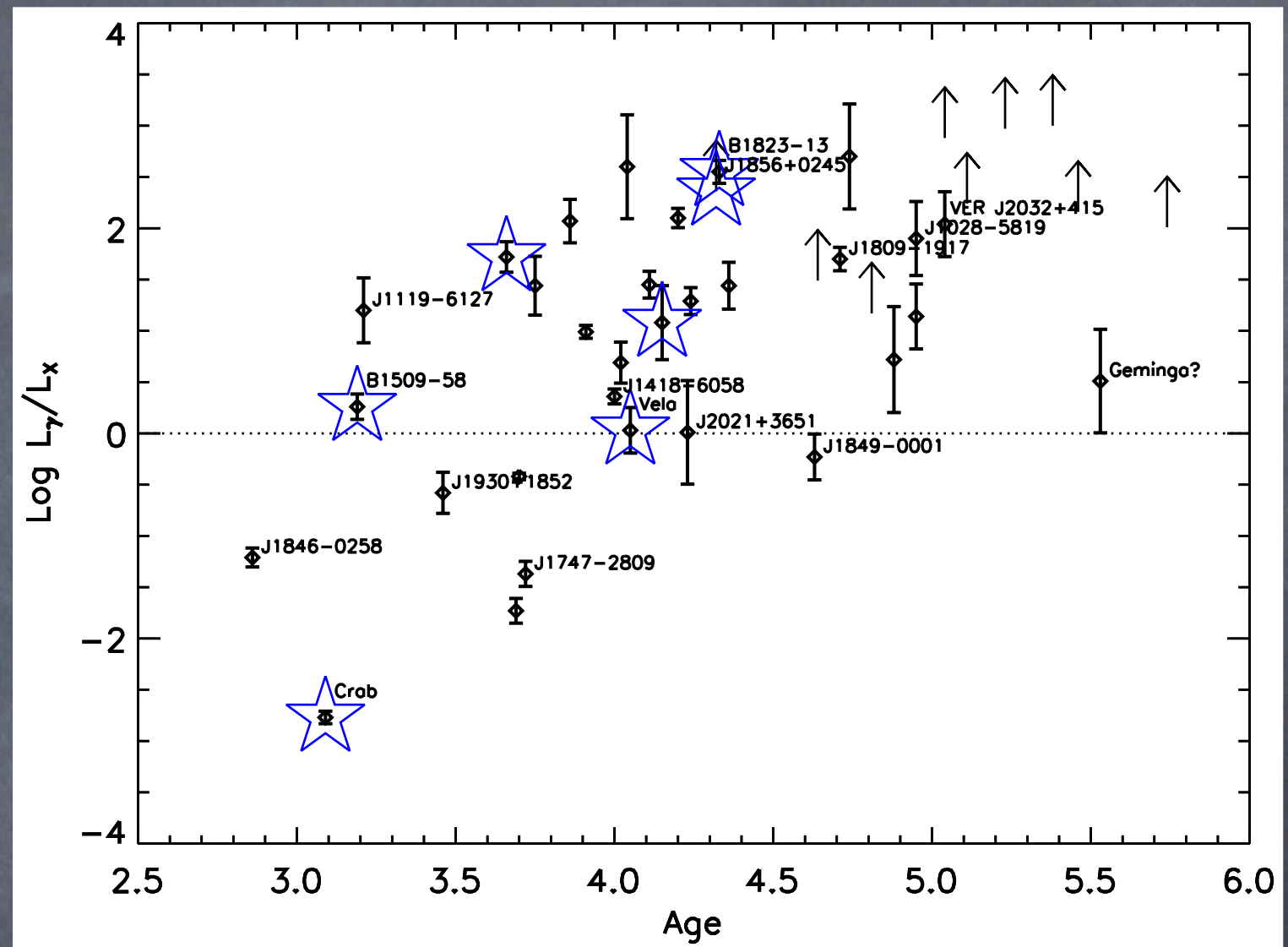
X-ray luminosities of PWNe and PWN candidates vs. pulsar's \dot{E} . TeV PWNe and TeV PWN candidates are shown in red. The dotted straight lines correspond to constant X-ray efficiencies; the upper bound, $\log L_X^{CR} = 1.51 \log \dot{E} - 21.4$, is shown by a dashed line. The PWNe detected in GeV by Fermi are marked by stars.



TeV luminosities of PWNe and PWN candidates vs. pulsar's \dot{E} (left) $\dot{E}^{1/2} T_{SD}$ (right). Thin error bars mark questionable associations. The PWNe undetected in X-rays are marked by circles. PWNe detected by Fermi are marked by stars.

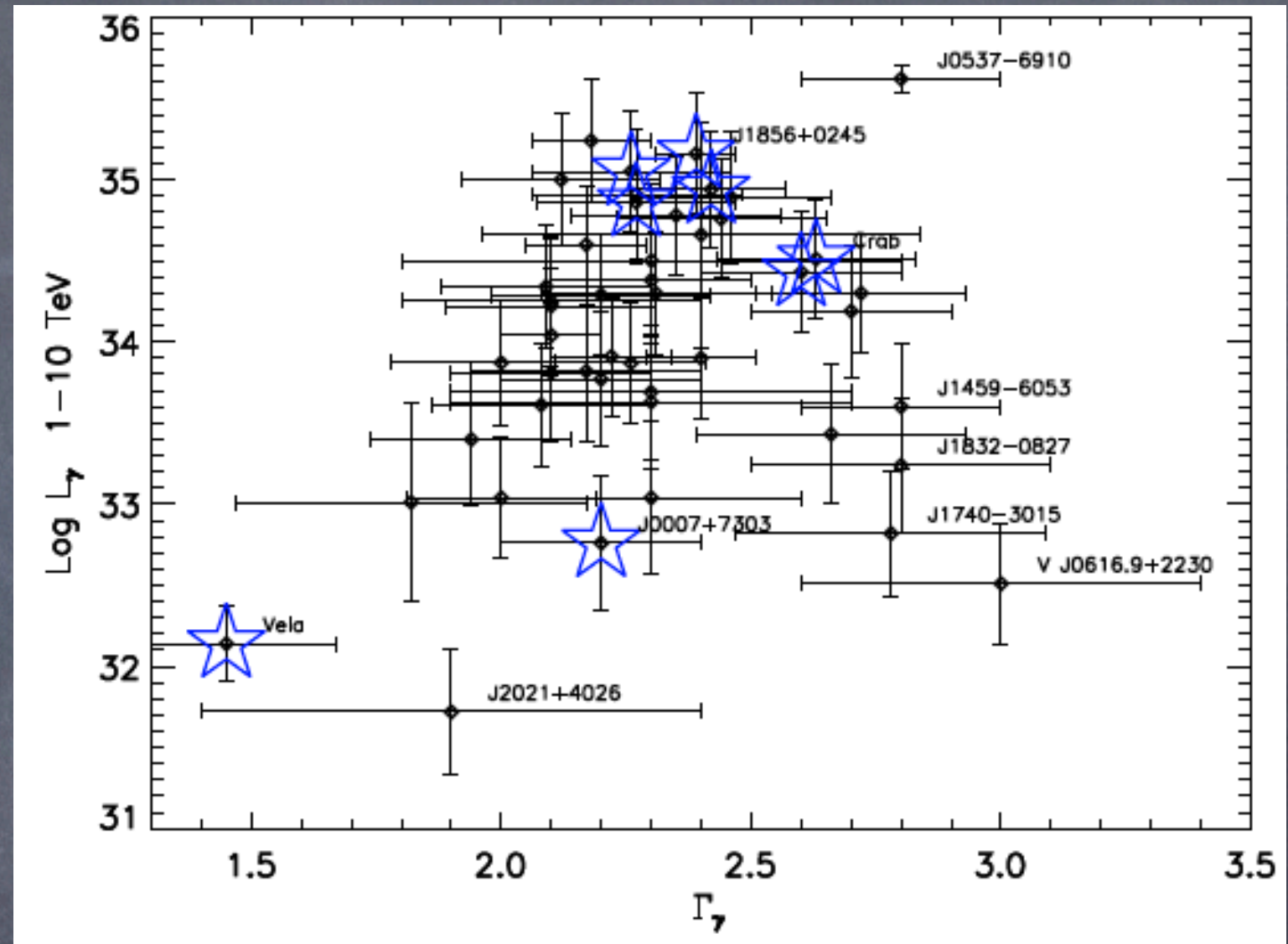
- TeV luminosities do not show significant correlation with \dot{E}
- No correlation between L_{γ} and $\dot{E}^{1/2} T_{SD}$
- Varying pair production, deviation from dipolar magnetic field, different environmental conditions, possible interaction with SNR reverse shock

- L_γ/L_X is distance independent
- The substantial scatter is not due to distance errors
- The correlation is similar in shape to the simplistic one-zone PWN model (de Jager et al. 2009), which may not be relevant for relic PWNe (significantly displaced)



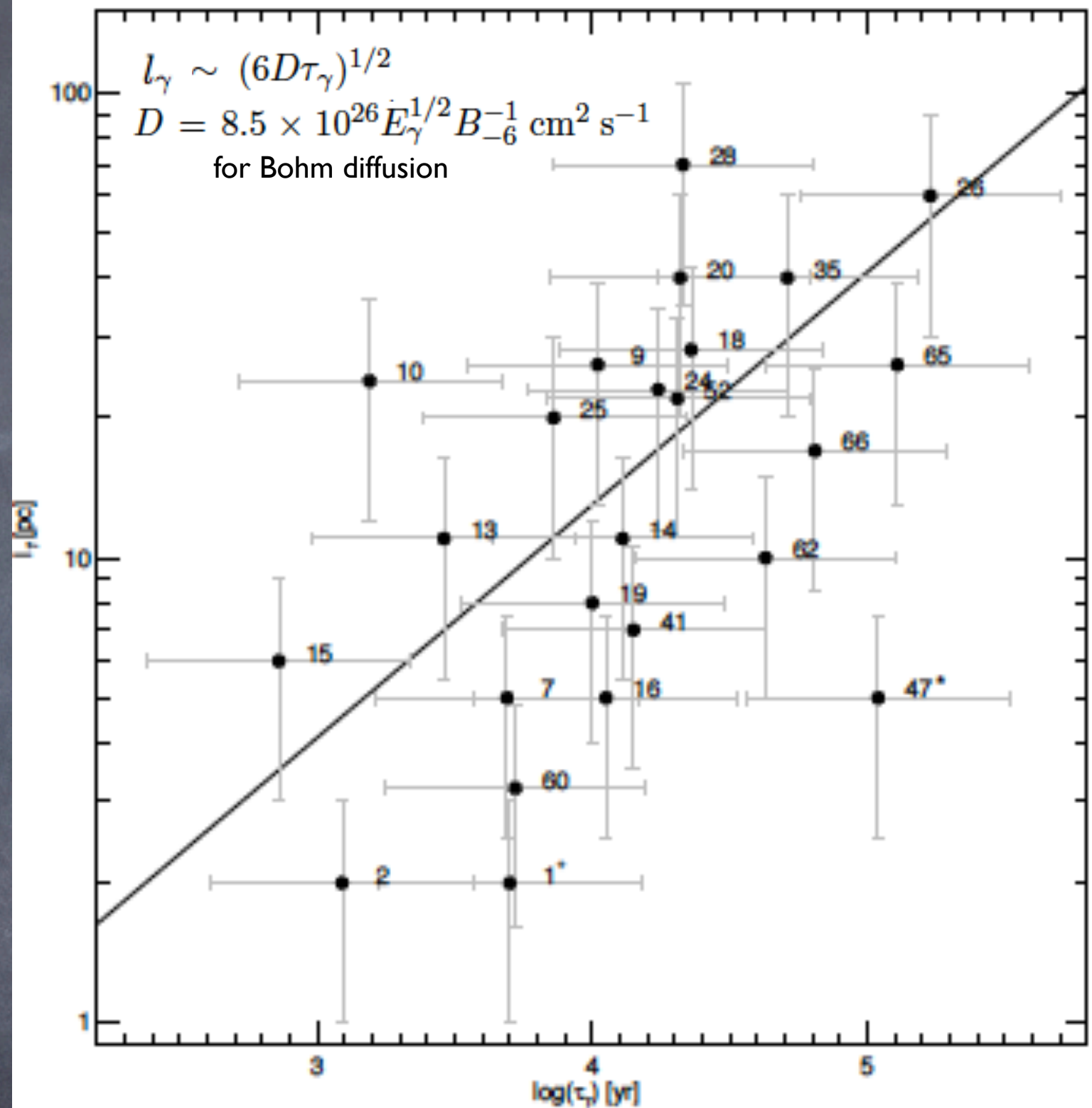
TeV-to-X-ray luminosity ratio vs. pulsar's age for PWNe and PWN candidates. Limits are shown by arrows. The PWNe detected by Fermi are marked by stars. Uncertain detections are shown by thin lines. The dotted lines corresponds to $L_\gamma = L_X$

- In most cases TeV PWN spectra fit well with power-law model
- Spectral cutoffs at > 10 TeV are seen in some cases
- Γ_γ increases with L_γ up to $L_\gamma \sim \text{a few } \times 10^{35} \text{ erg/s}$, then the trend is reverse (more precise measurements are needed)



TeV PWN luminosity vs. photon index. PWNe detected by Fermi are marked by stars.

- In “relic” PWNe particle escape via diffusion can be more important than advection
- Bohm diffusion prediction comparable to observed sizes of some VHE sources



Size of the TeV emission region (for firmly established TeV PWNe) as a function of pulsar's spin-down age. The straight line represents the characteristic size, corresponding to diffusion with the Bohm diffusion coefficient D . Source 1 (marked with +) is located in the Large Magellanic Cloud. Source 47 (marked with *) may have its distance underestimated by a factor of 2.

PWNe phenomenology

- Very young PWNe powered by energetic pulsars
 - No significant offset of the X-ray PWNe from the pulsars
 - γ -rays and X-rays likely emitted by same population of electrons
- Older objects
 - TeV PWNe much larger than (and often strongly offset from) X-ray PWNe
 - Compressed by SNR reverse shock and filled with aged electrons

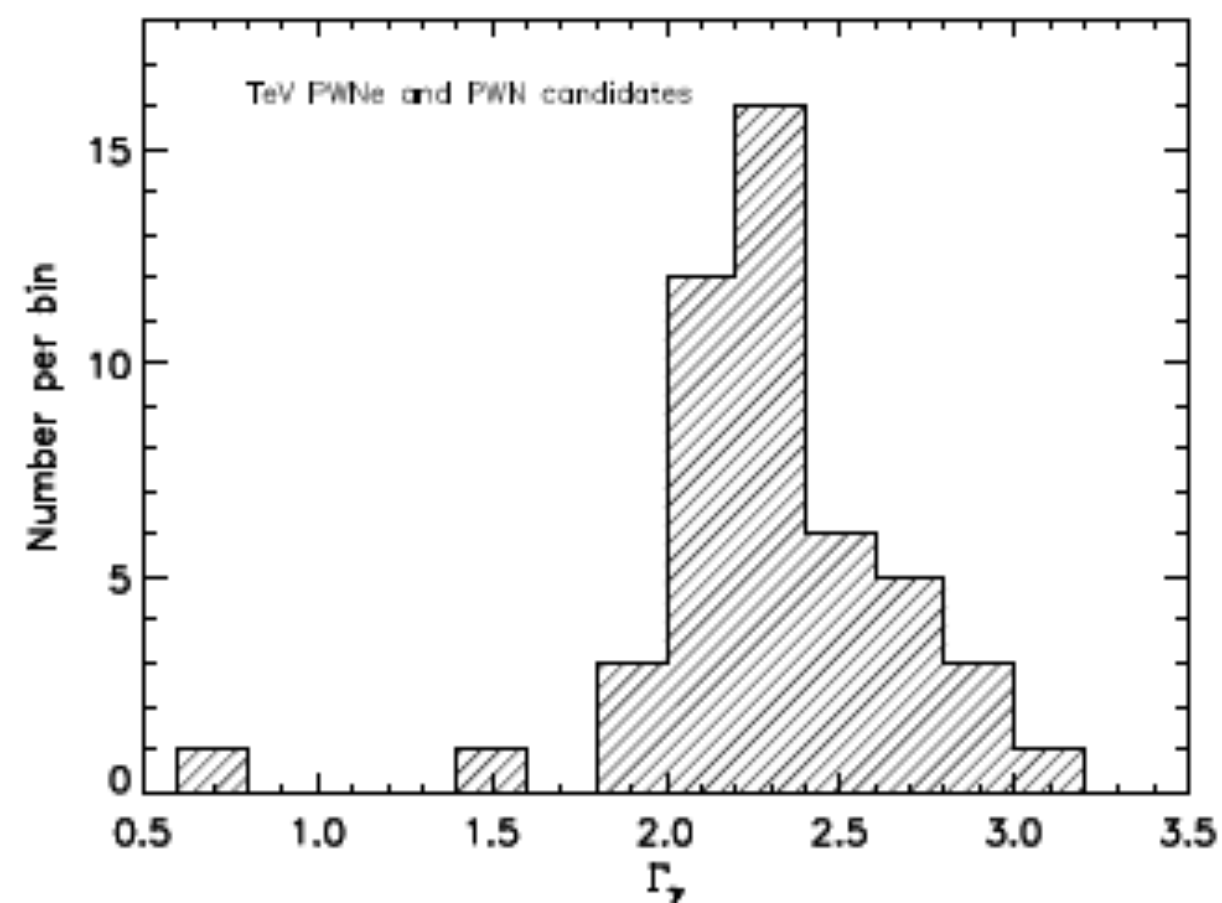
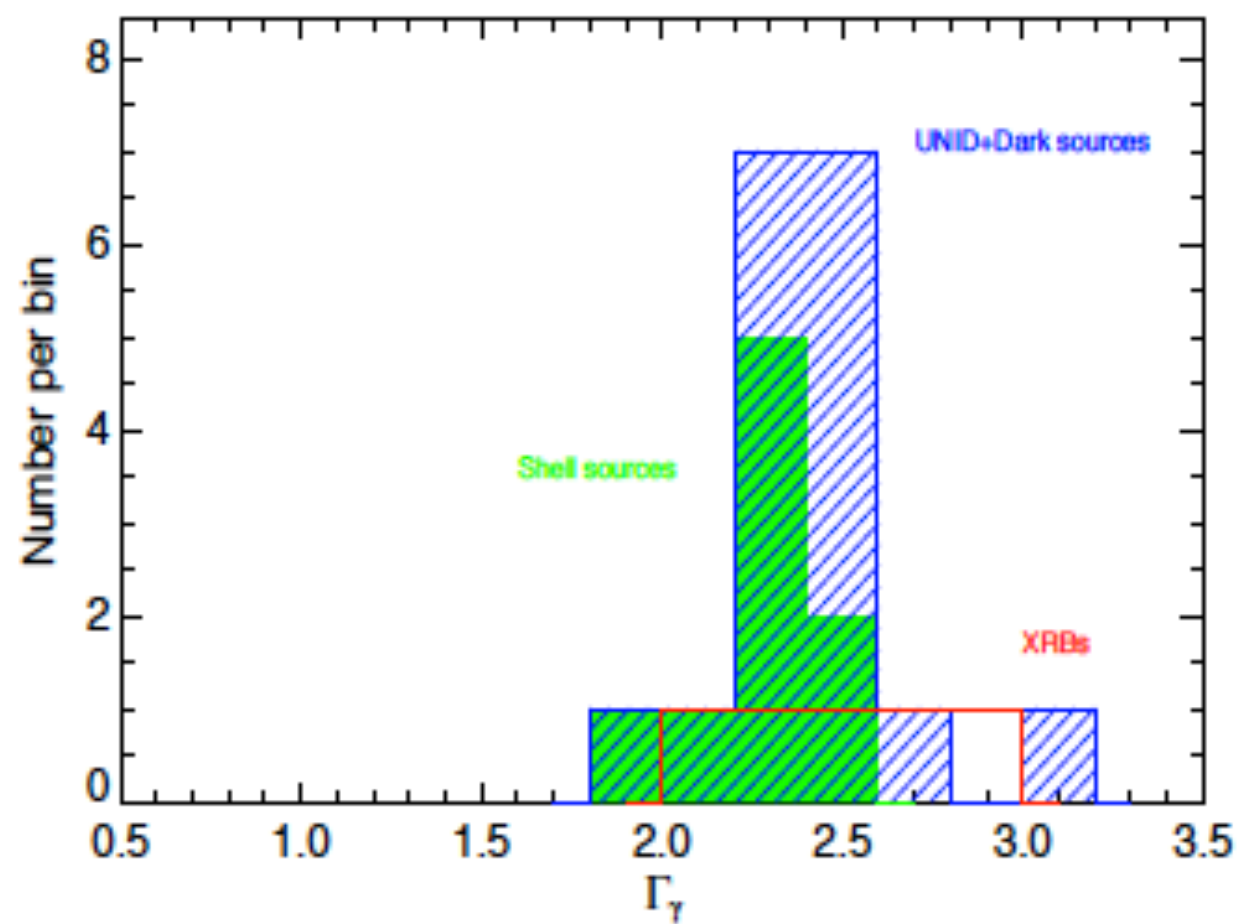
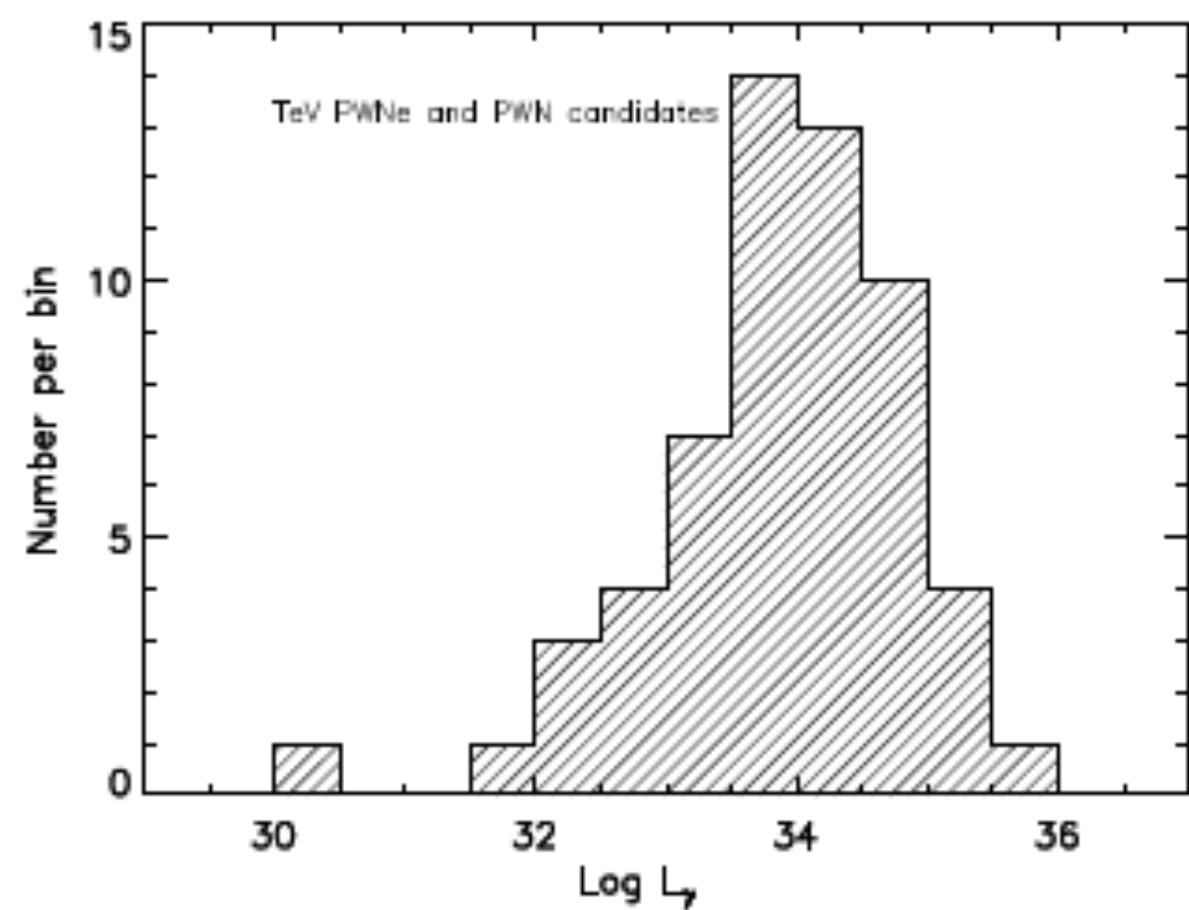
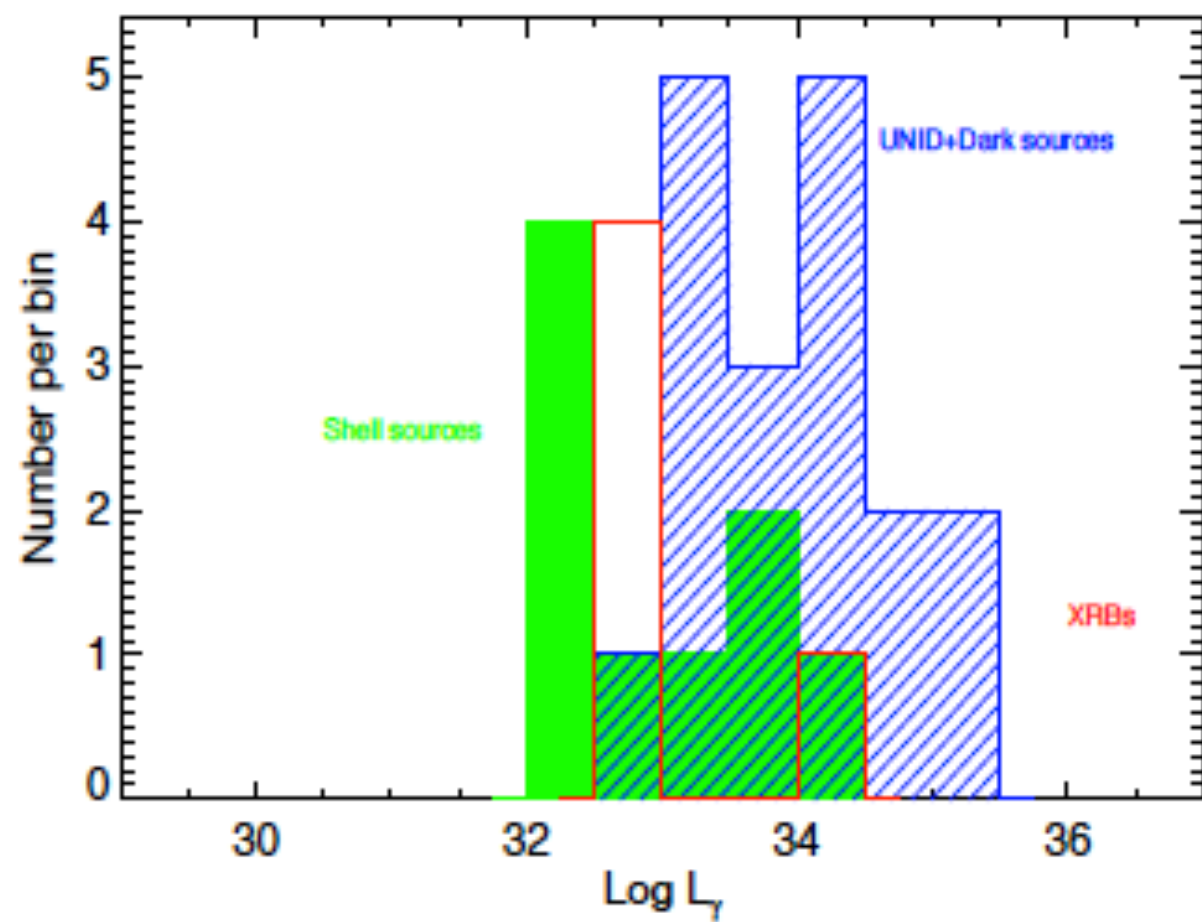
SNR shells and HMXBs detected in TeV

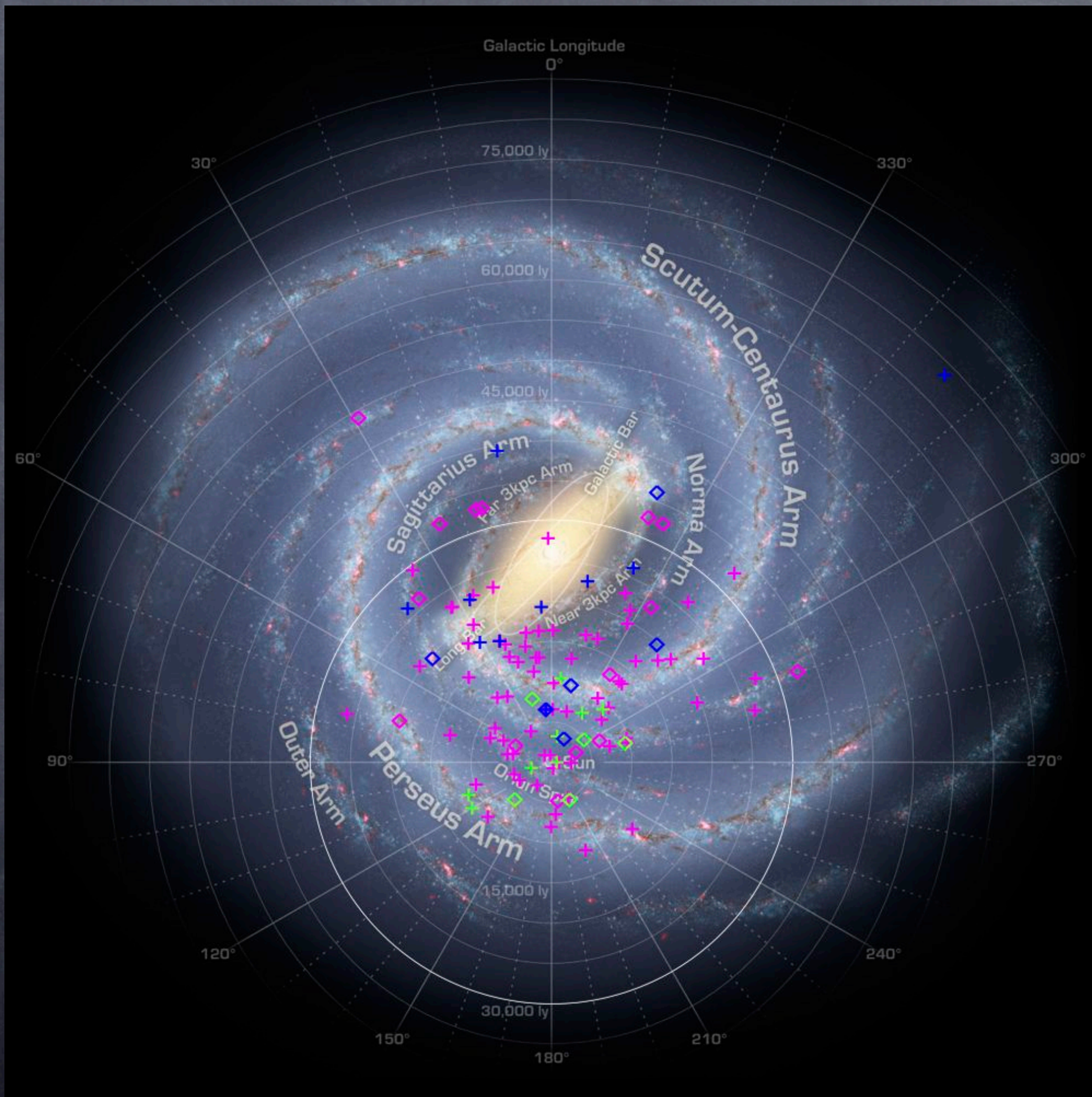
- Most shells are resolved in TeV images
- VHE emission associated with forward shock
- None of the SNRs hosts a pulsar, but some host central compact object
- The origin of VHE emission from SNR shells is still an open question. Both leptonic and hadronic mechanisms are still actively discussed
- Two types: binaries where a rotation-powered pulsar interacts with the strong wind of the massive stellar companion (SS 2883/B1259-63 and, likely, HESS J0632+057) and microquasars (LS 5039 and LS I +61 303)

| # | TeV Source | l^a deg | b^a deg | d kpc | $\log L_\gamma^b$ [erg/s] | Γ_γ | α^c deg | Ref. |
|----------------|------------------|--------------|--------------|------------|------------------------------|-----------------|-------------------|------------|
| Shells | | | | | | | | |
| 1 | HESS J1731-347 | 353.57 | -0.62 | 3.2 | 34.25 | 2.26 | 0.18/0.11 | [57] |
| 2 | Tycho | 120.11 | 1.45 | 3.5 | 32.22 | 1.95 | 0.11 | [135] |
| 3 | HESS J0852-463 | 266.28 | -1.24 | 0.2 | 32.31 | 2.24 | 1 | [136] |
| 4 | HESS J1442-624 | 315.41 | -2.30 | 2.8 | 33.87 | 2.54 | 0.45 | [137] |
| 5 | HESS J1502-421 | 327.86 | 15.35 | 2.2 | 32.38 | 2.29 | 0.5 | [138] |
| 6 | HESS J1504-418 | 327.84 | 14.56 | 2.2 | 32.53 | 2.35 | 0.5 | [138] |
| 7 | HESS J1713-397 | 347.34 | -0.47 | 1.0 | 33.72 | 2.19 | 0.65 | [139, 140] |
| 8 | VERJ2227+608 | 106.35 | 2.71 | 0.8 | 32.41 | 2.29 | 0.27/0.18 | [141] |
| 9 | Cas A | 111.71 | -2.13 | 3.4 | 33.24 | 2.50 | Unresolved | [142] |
| 10 | HESS J1729-345 | 353.44 | -0.13 | 3.2 | 33.18 | 2.24 | 0.14 | [143] |
| X-ray Binaries | | | | | | | | |
| 11 | HESS J0632+057 | 205.66 | -1.44 | 1.6 | 32.77 | 2.53 | Unresolved | [144, 145] |
| 12 | SS 2883/B1259-63 | 304.19 | -0.99 | 1.5 | 32.90 | 2.92 | Unresolved | [146] |
| 13 | LS 5039 | 16.90 | -1.28 | 2.5 | 34.09 | 2.12 | Unresolved | [147] |
| 14 | LS I +61 303 | 135.67 | 1.09 | 2.0 | 32.93 | 2.4 | Unresolved | [148] |
| 15 | HESS J1018-589A | 284.26 | -1.82 | 2.9 | 32.89 | 2.70 | Unresolved | [74] |

Unidentified and “dark” TeV sources

| # | TeV Source | l^a deg | b^a deg | d kpc | $\log L_\gamma^b$ [erg/s] | Γ_γ | α^c deg | Δ_{2FGL}^d arcmin | Δ_{ATNF}^e arcmin | X-ray ^f | Suggested type |
|----------------------|-----------------|--------------|--------------|------------|------------------------------|-----------------|-------------------|-----------------------------|-----------------------------|---------------------|-------------------|
| Unidentified Sources | | | | | | | | | | | |
| 1 | HESS J1800-240C | 5.71 | -0.06 | 2.0 | 32.90 | 2.31 | Unresolved | 0.53 | ... | ... | SNR/MC |
| 2 | HESS J1800-240A | 6.14 | -0.63 | 2.0 | 33.18 | 2.55 | 0.15 | 16.04 | ... | ... | SNR/MC |
| 3 | HESS J1911+090 | 43.26 | -0.19 | 8.0 | 33.37 | 3.10 | Unresolved | 0.97 | ... | Ch:Diffuse | SNR/MC |
| 4 | HESS J1729-345 | 353.44 | -0.13 | 3.2 | 33.18 | 2.24 | 0.14 | ... | ... | ... | UNID |
| 5 | HESS J1808-204 | 9.93 | -0.10 | 12.0 | 34.00 | 2.40 | ext | 15.40 | 9.39 | Ch&XMM:mult.pt.src. | Magnetar |
| 6 | HESS J1841-055 | 26.79 | -0.20 | 6.9 | 35.21 | 2.41 | 0.41/0.25 | 28.29 | 16.17 | Yes | PWN/Binary? |
| 7 | HESS J1713-381 | 348.65 | 0.38 | 7.0 | 33.86 | 2.65 | Unresolved | 18.96 | 1.93 | Ch:Diffuse+pt.src. | Shell/Magnetar |
| 8 | HESS J1834-087 | 23.26 | -0.33 | 5.0 | 34.37 | 2.50 | Unresolved | 8.82 | 0.90 | XMM:Diffuse+pt.src. | PWN/Magnetar |
| 9 | HESS J1427-608 | 314.41 | -0.14 | 21.0 | 35.29 | 2.16 | Unresolved | 3.07 | ... | XMM:mult.pt.src. | UNID |
| 10 | HESS J1747-248 | 3.78 | 1.72 | ... | ... | ... | | 2.74 | 8.45 | Ch:mult.pt.src. | Terzan 5 |
| 11 | HESS J1634-472 | 337.00 | 0.22 | 8.0 | 34.57 | 2.38 | 0.11 | 9.53 | ... | ... | UNID |
| 12 | HESS J1848-018 | 31.00 | -0.16 | 5.3 | 33.84 | 2.80 | 0.32 | 9.01 | ... | ... | UNID |
| 13 | HESS J1457-593 | 318.36 | -0.43 | ... | ... | ... | 0.31/0.17 | ... | ... | ... | SNR/MC |
| Dark Sources | | | | | | | | | | | |
| 14 | HESS J1923+141 | 49.13 | -0.40 | 6.0 | 34.54 | 2.60 | ext | 3.79 | ... | Ch:mult.pt.src. | SNR/MC |
| 15 | HESS J1800-240B | 5.96 | -0.38 | 2.0 | 32.89 | 2.50 | 0.15 | 2.76 | ... | Ch:mult.pt.src. | SNR/MC |
| 16 | HESS J1843-033B | 29.03 | 0.37 | ... | ... | ... | ext | 11.80 | 13.13 | Ch:mult.pt.src. | UNID |
| 17 | HESS J1614-518 | 331.51 | -0.57 | 1.0 | 33.34 | 2.26 | 0.23/0.15 | 14.27 | ... | Ch:mult.pt.src. | UNID |
| 18 | HESS J1507-622 | 317.95 | -3.49 | 6.0 | 34.26 | 2.24 | 0.15 | 3.25 | ... | Ch:Diffuse | UNID |
| 19 | HESS J1708-410 | 345.68 | -0.47 | 3.0 | 33.80 | 2.46 | Unresolved | ... | ... | XMM:mult.pt.src. | UNID |
| 20 | HESS J1641-463 | 338.52 | 0.09 | 11.0 | 34.22 | 1.99 | Unresolved | 15.56 | ... | Ch:mult.pt.src. | UNID |





Pulsars with detected PWNs and PWNs without detected pulsars are shown with crosses and diamonds, respectively, in magenta. Shells and HMXBs are shown with green crosses and diamonds, respectively. Unidentified and "dark" sources are shown with blue crosses and diamonds respectively.

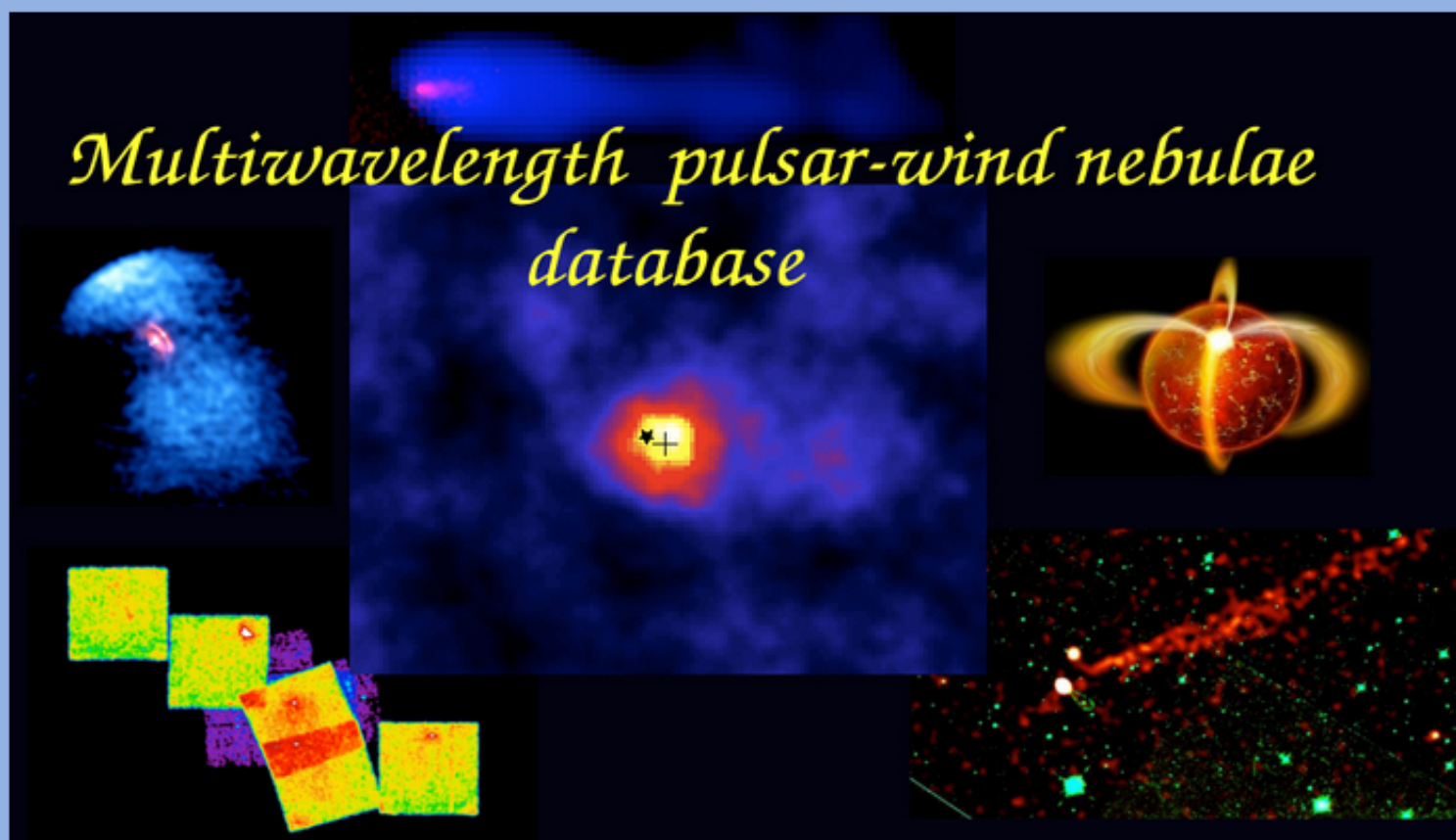
Multiwavelength pulsar-wind nebulae database

[Home](#) | [Pulsar Database](#) | [PWN Database](#)

[Login](#) | [Register](#)

Database currently contains 101 pulsars and 56 PWN.

Click the links above to visit the Pulsar or PWN database pages. Register and login on the left to new add sources to the database.



[Click here for dark and unidentified TeV sources](#)

Summary

- Most extended TeV sources appear to be relic PWNe because they are coincident with young and middle-aged pulsars which have X-ray PWNe. Chance coincidence is unlikely given the large number of cases.
- The VHE emission mechanism is likely to be ICS by PWN electrons, however hadronic contribution is not yet completely ruled out
- What are those “dark” UNIDed VHE sources? PWNe whose X-ray emission faded away? Plausible, but not established yet!
- The key to the identifications of “dark” TeV sources is a multiwavelengths follow-up and source classification.

Thank you!